

A versatile method for simulating $pp \rightarrow ppe^+e^-$ and $dp \rightarrow pne^+e^-p_{\text{spec}}$ reactions

I. Fröhlich², F. Dohrmann¹, T. Galatyuk², R. Holzmann³, P.K. Kähligt¹, B. Kämpfer¹, E. Morinière⁴, Y.C. Pachmayer², B. Ramstein⁴, P. Salabura^{3,5}, J. Stroth^{2,3}, R. Trebacz⁵, J. Van de Wiele⁴, and J. Wüstenfeld¹

¹ Institut für Strahlenphysik, Forschungszentrum Dresden-Rossendorf, 01314 Dresden, Germany

² Institut für Kernphysik, Goethe-Universität, 60438 Frankfurt, Germany

³ GSI Helmholtzzentrum für Schwerionenforschung GmbH, 64291 Darmstadt, Germany

⁴ Institut de Physique Nucléaire d'Orsay, CNRS/IN2P3, 91406 Orsay Cedex, France

⁵ Smoluchowski Institute of Physics, Jagiellonian University of Cracow, 30-059 Kraków, Poland

Abstract

We have developed a versatile software package for the simulation of di-electron production in pp and dp collisions at SIS energies. Particular attention has been paid to incorporate different descriptions of the Dalitz decay $\Delta \rightarrow Ne^+e^-$ via a common interface. In addition, suitable parameterizations for the virtual bremsstrahlung process $NN \rightarrow NNe^+e^-$ based on one-boson exchange models have been implemented. Such simulation tools with high flexibility of the framework are important for the interpretation of the di-electron data taken with the HADES spectrometer and the design of forthcoming experiments.

1 Introduction

Experiments with the High Acceptance Di-Electron Spectrometer (HADES) [1] are aimed at searching for medium modifications of hadrons at high density and moderate temperatures created in heavy-ion collisions in the 1-2 AGeV impact beam energy range. There exist a multitude of predictions, partially conflicting in details, awaiting verification or falsification [2, 3]. Due to negligible final-state interactions with nuclear matter, di-electrons or di-muons are considered to be useful penetrating probes for this purpose.

While at higher energies various experimental set-ups for di-lepton measurements have been or are operating, *e.g.*, HELIOS-3, CERES/NA35, NA38, NA50, NA60 (the latter three for di-muons), and PHENIX, HADES is the only presently active installation in the relativistic regime. In addition, it can cover elementary hadron reactions (pp , πp , and via tagging a spectator, also pn) and hadron–nucleus (pA , πA) collisions. This large range of reactions is related to the capabilities of the SchwerIonen-Synchrotron SIS18 at GSI, Darmstadt.

When searching for medium modifications of hadrons in the di-electron channel, it is important to have a reliable experimental reference, in particular from elementary hadronic reactions.

This became clearly evident in view of the unexplained pair excess measured by the DLS and, more recently, HADES experiments [4, 5]. In addition, the knowledge of the elementary process $NN \rightarrow NNe^+e^-$ is a prerequisite to understand possible in-medium effects in heavy-ion dilepton data [3, 6]. In this context, HADES has performed two di-electron experiments using a liquid hydrogen target and proton/deuteron beams [7, 8]: pp at 1.25 GeV and dp at 1.25 AGeV, *i.e.*, at the same kinetic beam energy per nucleon, which access a broad range of topics. For example, the branching ratio and involved electromagnetic transition form factors of the Δ Dalitz decay ($\Delta \rightarrow N\gamma^* \rightarrow Ne^+e^-$) are unmeasured. In particular, the di-electron production in the NN collision is regarded to be sensitive to the nucleon form factor in the time-like region [9, 10]. Moreover, the cross section of non-resonant virtual photon emission (often referred to as “bremsstrahlung”) differs by up to a factor 4 in the most recent calculations [11, 12, 13].

On the other hand, the different contributions of short-lived sources are not easy to separate, as, in principle, they have to be treated in a coherent approach, which is done usually in quantum mechanical calculations including the interferences, using *e.g.* One-Boson Exchange (OBE) models. Such calculations for the process $NN \rightarrow NNe^+e^-$ have already been done in [14] and more recently in refs. [11, 12, 13].

Our goal is to present the methods and their applicability to the HADES pp/pn data in order to have a simulation tool at our disposal to be sensitive to additional sources going beyond the Δ Dalitz decay contribution. Due to restricted phase space coverage and efficiency, a flexible simulation tool, which is capable to make direct comparison of model predictions with data is particularly useful in this respect. Here we describe an extended version of the event generator Pluto [15] which is the standard simulation tool for the HADES experiments.

The calculations mentioned above ensure a coherent treatment of the $NN \rightarrow NNe^+e^-$ reaction, including graphs involving nucleons, Δ 's or higher resonances and fulfill gauge invariance. As the graph involving the Δ Dalitz decay process is expected to be dominant in the pp reaction and still important in the pn reaction, a separate treatment of this contribution is useful. Therefore, one has to consider two mechanisms for simulations: either a full calculation including properly the interference effects, or the production via resonances (*e.g.* the $\Delta(1232)$) and their subsequent decay, the so called Δ Dalitz decay model.

Following these aims a versatile simulation framework has to be able to:

1. convert parameterized (or calculated) differential cross sections of the $NN \rightarrow NNe^+e^-$ reaction into “exclusive” events and, alternatively,
2. produce di-electrons via resonances ($NN \rightarrow \Delta N \rightarrow NNe^+e^-$) using mass-dependent branching ratios and angular distributions.

For each of these two methods different descriptions should be compared. These new developments are useful wherever simulations of this kind (in NN as well as in future πN experiments) have to be done in the context of the interpretation of HADES data.

The main goal of this report is to describe a standardized method to incorporate calculations for $NN \rightarrow NNe^+e^-$ reactions wherever available and subsequently to compare them to experimental data using an open-source and adaptable package, and to demonstrate how simulations of the dp/pp reaction may be performed to provide a valuable tool for interpreting the

HADES data [8]. Our paper is organized as follows. In section 2, we outline the numerical implementation, the software framework and how the simulation of both types have been done. The simulation results are discussed in section 3. Our summary can be found in section 4. In appendix A, we explain the models included to describe the Δ Dalitz decay and the used form factors.

2 Numerical realization

2.1 Pluto framework

The simulations which are presented here have been elaborated within the context of the Pluto framework [15] originally intended to be used for experiment proposals. The Pluto package is entirely based on ROOT [16] and steers the event production with very little overhead by using so-called “macros” which are - within the ROOT framework - based on the C++ language.

After the set-up procedure, the event loop is called N_{ev} times which creates the momenta of all involved particles (and masses in the case of unstable ones) event-by-event. Subsequently, each event is usually filtered with the detector acceptance or fed into a full digitization package like Geant [17] (not part of our package). The pp (or pn) system enters - in our case - as a “seed object” into the decay chain with a given center of momentum (c.m.) total energy and momentum. Cocktails - which are the incoherent sum of different reaction channels - can be generated as well.

Recently, the Pluto package was re-designed in order to introduce a more modular, object-oriented structure, thereby making additions such as new particles, new decays of resonances and new algorithms up to modules for entire changes (plug-ins) easily applicable [18].

2.2 The Δ mass shape

One method of event-based simulations is to set up a reaction of consecutive decays, like $pp \rightarrow p\Delta^+ \rightarrow pp\gamma_{ee}^* \rightarrow ppe^+e^-$. Hence, this means that the Δ mass shape (and mass-dependent branching ratios) must be known prior to event sampling.

How does one usually generate N_{ev} events for the Dalitz decay $\Delta \rightarrow N\gamma_{ee}^*$? In the first step, the Δ mass shape is sampled, *i.e.*, for each event i , a mass $m_{\Delta}^{(i)}$ is assigned.

Following the usual ansatz (see *e.g.* [19]) we use the relativistic form of the Breit Wigner distribution:

$$g^{\Delta}(m_{\Delta}) = A \frac{m_{\Delta}^2 \Gamma^{\text{tot}}(m_{\Delta})}{(M_{\Delta}^2 - m_{\Delta}^2)^2 + m_{\Delta}^2 (\Gamma^{\text{tot}}(m_{\Delta}))^2} \quad (1)$$

where m_{Δ} denotes the actual energy (resonance mass), and M_{Δ} is the static pole mass of the resonance. The mass-dependent width is the sum of the partial widths

$$\Gamma^{\text{tot}}(m_{\Delta}) = \sum_k^N \Gamma^k(m_{\Delta}) \quad (2)$$

with N the number of decay modes. The factor A is chosen such that the integral is statistically normalized, $\int dm_\Delta g^\Delta(m_\Delta) = 1$, i.e., eq. (2) leads to the following condition for the mass-dependent branching ratio for each decay mode k

$$b^k(m_\Delta) = \frac{\Gamma^k(m_\Delta)}{\Gamma^{\text{tot}}(m_\Delta)}. \quad (3)$$

The width for the dominating hadronic decays $\Delta \rightarrow N\pi$ is derived from a well-known ansatz [19, 20, 21]:

$$\begin{aligned} \Gamma^{\Delta \rightarrow N\pi}(m_\Delta) &= \frac{M_\Delta}{m_\Delta} \left(\frac{q^\pi(m_\Delta)}{q^\pi(M_\Delta)} \right)^3 \\ &\times \left(\frac{\nu(m_\Delta)}{\nu(M_\Delta)} \right) \Gamma^{\Delta \rightarrow N\pi}. \end{aligned} \quad (4)$$

The dependence on the two decay products with masses m_N and m_π enters via the terms $q^\pi(m_\Delta)$ and $q^\pi(M_\Delta)$, namely the momentum of one out of the two decay products in the rest frame of the parent resonance. We follow ref. [19, 21] which uses for the resonance the cutoff parameterization

$$\nu(m_\Delta) = \frac{\beta^2}{\beta^2 + (q^\pi(m_\Delta))^2} \quad (5)$$

with the parameter $\beta=300$ MeV.

To simulate the Dalitz decay, the mass-dependent branching ratio has to be taken into account as

$$g^{\Delta \rightarrow Ne^+e^-}(m_\Delta) = b^{\Delta \rightarrow Ne^+e^-}(m_\Delta) g^\Delta(m_\Delta). \quad (6)$$

Thus, the partial decay width

$$\Gamma^{\Delta \rightarrow Ne^+e^-}(m_\Delta) = \int dm_{ee} \frac{d\Gamma^{\Delta \rightarrow Ne^+e^-}}{dm_{ee}} \quad (7)$$

has to be used in the numerator of eq. (1) which is calculated by integrating eq. (7) with a small step size for each m_Δ mass bin, respectively.

The differential Δ Dalitz decay width $d\Gamma/dm_{ee}$ depends on three transition form factors, as explained in more detail in the appendix. In particular, we compare the effect of using constant form factors, with same values as for a real photon emission (“photon-point” form factors) with a two-component model from Iachello and Wan [22] which is in line with the vector-meson dominance (VMD) model. This leads to different mass shapes $g^{\Delta \rightarrow Ne^+e^-}(m_\Delta)$ which is exhibited in Fig. 1.

One can see that the mass-dependent branching ratio decreases with mass. This feature is an important issue for the di-electron production as large contributions of the higher-mass tail of the Δ resonance and the mass-dependence in the Δ Dalitz branching ratios affect not only the di-electron invariant-mass spectral shape but also the di-electron yield, compared to the hadronic channels. Therefore, the mass-dependent branching ratio must be considered even if the effect might be suppressed in part by the limited phase space.

How can an event generator take that behavior into account for the mass sampling? An elegant way by using the weighting method is explained in the next subsections.

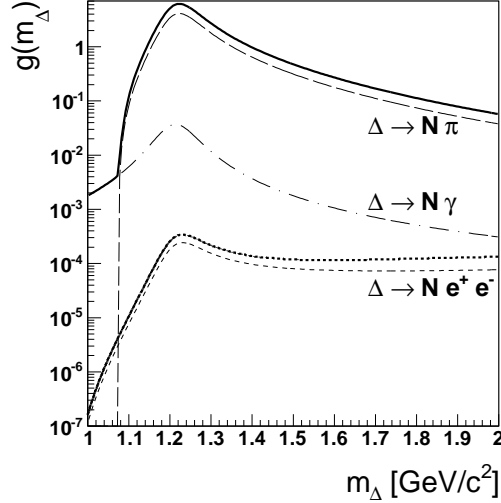


Figure 1: Free spectral shape g^Δ as a function of m_Δ of $\Delta^+(1232)$ (solid line) compared to the distribution functions for dedicated decay states. Short dashed line: $\Delta^+(1232) \rightarrow e^+e^-p$ (ref. [24] with “photon point” magnetic form factor), long dashed line: $\Delta^+(1232) \rightarrow \pi^0 + p$ and dashed-dotted line: $\Delta^+(1232) \rightarrow \gamma + p$. In addition, the effect of the two component quark-model transition form factor of ref. [22] is indicated by the short dotted line.

2.3 Weight-based method

Our first step is to bring the spectrum (represented by a histogram) onto an absolute scale such that one can assign each of its bins to a differential cross section. Therefore, total cross section models for elementary NN collisions have been implemented.

For the reactions discussed here, two major contributions (beside the bremsstrahlung) have been added, which is the Δ production [19] (we assume $\sigma_{pp \rightarrow p\Delta^+} = \frac{3}{2}\sigma_{pp \rightarrow pp\pi^0}$) and the close-to-threshold η production [25, 26, 27] (the latter one is needed for the pn case). In order to obtain these cross sections independent of the number of events, first a default weight of $1/N_{\text{ev}}$ is applied to the NN seed object. In the decay algorithms, where mass and momentum sampling takes place, the weights of all attached distributions are multiplied with the default weight of the parent particle to an event weight W_i . In particular, parameterizations for the total cross section can be included. This leads - in a 1-step decay as defined above - to the simple relation

$$\sigma^{NN \rightarrow XZ} = \sum_i^{N_{\text{ev}}} W_i = \frac{1}{N_{\text{ev}}} \sum_i^{N_{\text{ev}}} W^{NN \rightarrow XZ}, \quad (8)$$

where X is an unstable particle (e.g. π^0 , η) and Z stands for the remaining particles. Eq. (8) is the basic definition to be used in all weighted Pluto simulations: The integral (sum) of the resulting histogram weights represents the total (or partial) cross section of an exclusive reaction. Therefore, the simulated spectra can be compared directly to the normalized experimental data.

If we now extend this definition to a two-step process, where a decay $X \rightarrow ab$ follows, the weight of particle X has to be folded with the mass-dependent weight of the consecutive decay model, which will be described in Sec. 2.6.

In the simplest case we can consider that production and decay of X are independent, which is the case for the η as well as for the π^0 as they have a comparable small width. In particular, by using a sampling model (returning a random event from the known distributions and momenta of a, b) this weight is the static branching ratio $W^{X \rightarrow ab} = b^{X \rightarrow ab}$ yielding

$$\sigma^{NN \rightarrow abZ} = \frac{1}{N_{\text{ev}}} \sum_i^{N_{\text{ev}}} W^{NN \rightarrow XZ} b^{X \rightarrow ab}. \quad (9)$$

2.4 Flat di-electron generator

Very often experiments are concerned with regions of the phase space, where a small number of events is expected compared to the overall number of a given process. This is clearly the case for the electromagnetic Dalitz decays, where the di-lepton yield spans many orders of magnitude with a high differential cross section for the low-mass pairs, whereas the high-mass pairs have a much lower cross section $d\sigma/dm_{ee}$. Obviously, a large number of events have to be sampled before an acceptable number in the high-mass region has been collected. On the other hand, the Monte-Carlo simulations presented here need an adequate statistics for the high-mass region of interest.

The solution used here is that sampling is done using a flat di-lepton distribution first. Then, a weight is calculated using the same physics decay model, which was employed for the sampling in Sec. 2.2. This means, the decay weight $W_i^{X \rightarrow ab}$ changes from event to event, depending on the values $m_i = m_{ee}^{(i)}$.

By extending eq. (9) we get for the Dalitz decays of the pseudo scalar mesons

$$\begin{aligned} \sigma^{NN \rightarrow NN e^+ e^- \gamma} &= \frac{1}{N_{\text{ev}}} \sum_i^{N_{\text{ev}}} W^{NN \rightarrow NN(\eta, \pi^0)} \\ &\times S^{(\eta, \pi^0) \rightarrow e^+ e^- \gamma} W^{(\eta, \pi^0) \rightarrow e^+ e^- \gamma}(m_{ee}^{(i)}) \end{aligned} \quad (10)$$

with $W^{(\eta, \pi^0) \rightarrow e^+ e^- \gamma}(m_{ee})$ as the differential cross section from [23]. The normalization factor

$$S^{(\eta, \pi^0) \rightarrow e^+ e^- \gamma} = b^{(\eta, \pi^0) \rightarrow e^+ e^- \gamma} / \overline{W^{(\eta, \pi^0) \rightarrow e^+ e^- \gamma}} \quad (11)$$

is used to normalize the spectrum to the selected branching ratio and thereby correct for the fact that more events are created in the phase space region with small probability, where the model weight is small compared to the region usually containing a large number of events. Here, the average decay weight

$$\overline{W^{(\eta, \pi^0) \rightarrow e^+ e^- \gamma}} = \frac{1}{N'_{\text{ev}}} \sum_{i=1}^{N'_{\text{ev}}} W_i^{(\eta, \pi^0) \rightarrow e^+ e^- \gamma}, \quad (12)$$

$$N'_{\text{ev}} = N_{\text{ev}} + N_{\text{pre}} \quad (13)$$

is first calculated for a selected number of events ($N_{\text{pre}} = 1000$ turned out to be sufficient to avoid artefacts) and then adjusted within the running event loop.

For broad resonances, as discussed in Sec. 2.2, the branching ratio should be an outcome, and no precondition of the calculation. The same argument can be brought forward for the calculations from refs. [11, 13]. Integrating these distributions is difficult since the underlying calculations are only presented for invariant di-electron masses larger than 50-100 MeV/c² [11, 13]. Thus, the partial cross section can not be calculated correctly and added to the data base; at least it would require some extrapolation. However, this can be avoided, as shown in the following.

2.5 Models returning $d\sigma/dm$

As an application for a simulation without an explicit re-normalization to a fixed branching ratio or total cross section, the above-mentioned weighting has been exploited because the calculations from refs. [11, 13] provide the differential cross section $d\sigma/dm_{ee}$ already done on an absolute scale. Aiming for a comparison of the Δ Dalitz decay with the resonant $N\Delta$ terms (method 1), we define as a model weight $W^{N\Delta}(m_{ee}^{(i)}) = d\sigma/dm_{ee}$ parameterized as described below. It is evident that the same method can be used for the full (coherent) differential cross section and the quasi-elastic term as well, just by replacing $W^{N\Delta}(m_{ee}^{(i)})$ in the generator by $W^{\text{full}}(m_{ee}^{(i)})$ and $W^{\text{ela}}(m_{ee}^{(i)})$, respectively.

In such a case it is more convenient to use the function $\frac{d\sigma}{dm_{ee}}$ directly with the flat di-electron distribution generator, as in the previous example, but without the intermediate step of production and decay. As the event loop generates a row of N_{ev} values $m_i = m_{ee}^{(i)}$ the cross section is represented naturally by the Monte-Carlo integration method as

$$\begin{aligned} \sigma^{pp \xrightarrow{N\Delta} ppe^+e^-} &= \int \frac{d\sigma}{dm_{ee}} dm_{ee} \\ &\approx \frac{1}{N_{\text{ev}}} \sum_{i=1}^{N_{\text{ev}}} W^{N\Delta}(m_{ee}^{(i)}) \cdot \Delta m_{ee}, \end{aligned} \quad (14)$$

where Δm_{ee} is the kinematic range of the di-electron generator (changing also event-by-event) which is provided by the model. It is an advantage that the normalization factor S is not needed.

The function $W^{N\Delta}$ required here has been obtained by digitizing the curves provided by ref. [11] and using a parameterization of the form

$$\begin{aligned} W^{N\Delta}(m_{ee}) &= \frac{d\sigma}{dm_{ee}}(m_{ee}) \\ &= \frac{(m_{\text{max}} - m_{ee})^{P_3}}{P_2 \exp(P_0 m_{ee} + P_1 m_{ee}^2)} \end{aligned} \quad (15)$$

with

$$m_{\text{max}} = \sqrt{(m_{N2} + m_{N1})^2 + 2m_{N2}T_{\text{kin}}} - (m_{N1} + m_{N2}) \quad (16)$$

as the kinematic limit with $N1$ as the beam nucleon. The parameters P_i fitted to the curves in ref. [11] are polynomials $P_i(T_{\text{kin}}) = a_i^0 \cdot a_i^1 T_{\text{kin}} \cdot a_i^2 T_{\text{kin}}^2$. The function $d\sigma/dm_{ee}$ of ref. [13] was directly supplied by the authors [28] for a fixed kinetic beam energy of $T_{\text{kin}} = 1.25$ GeV, and moreover of $T_{\text{kin}} = 1$ GeV and $T_{\text{kin}} = 1.5$ GeV for the pn case.

2.6 Models returning $d\Gamma/dm$

Let us continue with an alternative (method 2), where the Δ production is followed by the Dalitz decay. Pluto treats this process in two steps, leaving out the last and uncritical decay $\gamma_{ee}^* \rightarrow e^+e^-$. The weight $W^{\Delta \rightarrow N\gamma_{ee}^*}(m_\Delta, m_{ee})$ is now a function of two masses. Taking eqs. (3,7) the mass-dependent branching ratio is obtained by

$$b^{\Delta \rightarrow Ne^+e^-}(m_\Delta) = \int dm_{ee} \frac{d\Gamma_{m_\Delta}^{\Delta \rightarrow Ne^+e^-}(m_{ee})}{dm_{ee}} \frac{1}{\Gamma^{(\text{tot})}(m_\Delta)}. \quad (17)$$

Similar to eq. (14), the di-electron generator represents the Monte-Carlo integration method of the model

$$W^{\Delta \rightarrow N\gamma_{ee}^*}(m_\Delta, m_{ee}) = \frac{d\Gamma_{m_\Delta}^{\Delta \rightarrow Ne^+e^-}(m_{ee})}{dm_{ee}}. \quad (18)$$

Therefore the mass-dependent branching ratio obtained as

$$b^{\Delta \rightarrow Ne^+e^-}(m_\Delta) \approx \frac{1}{N_{\text{ev}}} \sum_{i=1}^{N_{\text{ev}}} \frac{W^{\Delta \rightarrow N\gamma_{ee}^*}(m_\Delta, m_{ee}) \cdot \Delta m_{ee}}{\Gamma^{(\text{tot})}(m_\Delta)} \quad (19)$$

is already considered, which means that the Δ mass shape has to be sampled in the first step with the pure function $g^\Delta(m)$ without using condition (6). This is ensured by the Pluto framework automatically. The effect of the mass dependence, as discussed in Sec. 2.2 becomes now visible: The fraction of the di-electron events, compared to the hadronic channels,

$$b(T_{\text{kin}}) = \frac{\sigma^{NN \rightarrow N\Delta \rightarrow NN e^+e^-}}{\sigma^{NN \rightarrow N\Delta}}, \quad (20)$$

is in our case with $b(T_{\text{kin}} = 1.25 \text{ GeV}) = 4.96 \cdot 10^{-5}$ significantly larger than the static branching ratio, which is $b^{\Delta \rightarrow Ne^+e^-} = 4.19 \cdot 10^{-5}$ (see A.2.1). This means that the mass-dependent branching ratio is an important feature which can not be neglected.

3 Simulation

3.1 Δ production

From the experimental point of view the consideration of known angular distributions is crucial. This is in particular true for the emission of the Δ resonance in the c.m. frame which affects

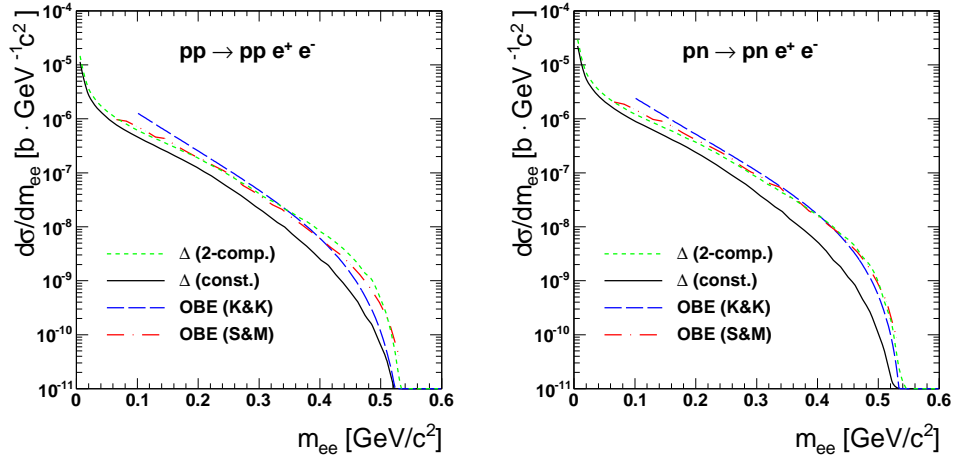


Figure 2: (color online) Resonant di-electron production in $Np \xrightarrow{N\Delta} Npe^+e^-$ reactions at $T_{\text{kin}}=1.25$ GeV. Left: pp reaction, Right: np reaction. The solid black curve and short-dashed (green) curves are the result of the full Pluto simulation using the mass-dependent Δ width, its production cross section and the $d\Gamma(m_\Delta)/dm_{ee}$ description from [24] with constant transition form factors (labeled with “const.”), the short-dashed (green) was obtained with the two component form factor [22] (labeled with “2-comp.”) in addition. The long-dashed (blue) curve is the calculation from [11], whereas the (red) dot-dashed curve is based on ref. [13] and provided by ref. [28].

the direction of both protons. The impact on the experimentally measured data comes due to the fact that the detection of the proton could be a trigger requirement or, explicitly, enters the analysis of a (semi-)exclusive channel, *e.g.* $pp \rightarrow Xpe^+e^-$. Such effects are often integrated out in calculations.

In the case of the Δ production, we follow the one-pion exchange model of ref. [29], which is in excellent agreement with the data and in detail described in ref. [15]. This adds a strong forward-backward peaking of the polar angle of the nucleons with respect to the beam axis, an effect which is considered in the two-step Dalitz decay simulations. In the OBE simulations virtual photons are generated with the differential cross sections taken from the coherent calculation like a hypothetical “on-mass” shell particle with a given mass m_{ee} . Due to missing information the momentum and energy is sampled assuming a three body phase space decay of the NN seed object sitting at rest in the center-of-mass with $m = m_{Np}$. Consequently, the virtual photons are emitted isotropically in the OBE, but not in the Δ simulation.

3.2 Different descriptions of the Δ Dalitz decay

After having all needed pieces at our disposal the difference between the OBE calculations [11, 13] and the calculations from [24] (either with the photon point form factors or the two component quark model option) can be studied in a quantitative way. Fig. 2 shows the Pluto

simulation for the processes $pp \rightarrow p\Delta^+ \rightarrow ppe^+e^-$ (left) and $pn \rightarrow N\Delta^{+,0} \rightarrow pne^+e^-$ (right) for the two descriptions mentioned above together with the resonant term $Np \xrightarrow{N\Delta} Npe^+e^-$ from the OBE calculation [11]. The two OBE calculations use the same $N - \Delta$ transition form factors, but the latter are different than the “photon point” form factors used in the two step Dalitz decay model. The effect on the di-electron spectrum is, however, expected to be lower than 15%.

It is obvious that the disagreement is much larger. The OBE calculation of ref. [11] is larger by a factor of 2-4 than the production via a “free” Δ using the mass-dependent branching ratio. The latter method is a crude approach, taking into account only one graph neglecting interferences and anti-symmetrization effects. It is, however, frequently used in transport code calculations.

The VMD calculation comes closer to the OBE model, but undershoots it at low masses as well. Surprisingly, we do not come to the same conclusion as ref. [13], where the spectrum of the two-step Dalitz decay model has a very steep slope. Qualitatively, our model is much closer to the OBE calculations of ref. [11, 13] and, taking the VMD form factor into account, lies almost on top the curves from ref. [13]. This clearly needs experimental confirmation and further theoretical studies.

3.3 Final state interaction

In all near-threshold reactions, the final state interactions (FSI) may influence strongly both the total cross section as well as the population of the phase space. The first effect is already included in the Delta Dalitz two-step simulation as they use measured data. For the OBE calculations the factorization [30, 31]

$$W^{\text{final}} = W^{\text{fsi}} \times W^{N\Delta, \text{full,ela}} \quad (21)$$

has been implemented. This is controlled via a switch which means a factor W^{fsi} is attached exploiting the inverse of the Jost function

$$W^{\text{fsi}} = \left(\frac{1}{J(k)} \right)^2 = \left(\frac{k + i\alpha}{k + i\beta} \right)^2 \quad (22)$$

with

$$\alpha, \beta = \frac{1}{r_0} \left(\sqrt{1 - \frac{2r_0}{a_0}} \pm 1 \right), \quad (23)$$

and k as the relative momentum of the two nucleons using the effective radii and scattering lengths $a_0 = -7.8098$ fm and $r_0 = 2.767$ fm for the pp case, and $a_0 = -23.768$ fm and $r_0 = 2.75$ fm for the pn case [31]. We use this description to be compatible with the calculation done in [11]; other functions could be implemented as well.

3.4 Nucleon momentum distribution in the deuteron

For the dp reaction, the nucleon momentum distribution in the deuteron has to be taken into account, because the effective neutron momentum may have a big impact at larger di-electron

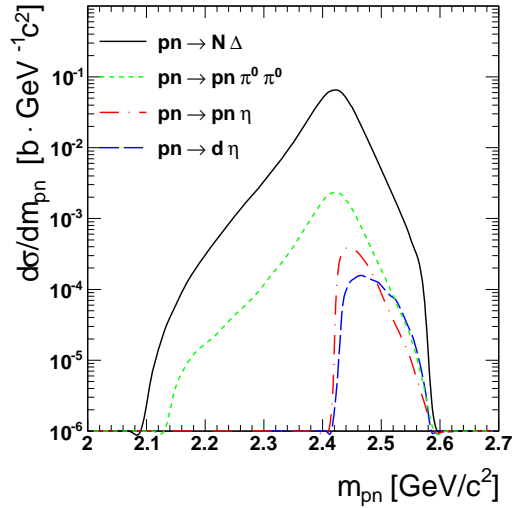


Figure 3: (color online) Differential cross section as a function of the invariant mass m_{pn} in the quasi-free pn reaction taking into account the deuteron momentum distribution. Solid curve: $\Delta^{+,0}$ production, short dashed (green) curve: $pn \rightarrow pn\pi^0\pi^0$ (constant $\sigma = 0.1$ mb assumed), long-dashed (blue) curve: $pn \rightarrow pn\eta$, dot-dashed (red) curve: $pn \rightarrow d\eta$.

masses [12]. This is done by Pluto in a two-step process. In the first step, the off-shell mass of the participant

$$m_{\text{part}}^2 = m_d^2 + m_p^2 - 2m_d \sqrt{m_p^2 + p_{\text{Deut}}^2} \quad (24)$$

is determined by the parameterized wave function p_{Deut} from ref. [32]. Along with the second reaction particle (in our case the target p at rest) this off-shell particle forms the pn composite with a total c.m. energy m_{pn} of the quasi-free reaction. In a second step the bremsstrahlung model calculates the energy

$$T_{\text{kin}} = \frac{m_{pn}^2 - m_p^2 - m_n^2 - 2m_p m_n}{2m_n} \quad (25)$$

of the proton in the neutron rest frame. Here, we use the invariant mass m_{pn} to get the total cross section $\sigma(m_{pn})$ using the on-shell neutron mass m_n , which is also the approach in ref. [33]. It is important to note that, as the di-electron cross section for the pn reaction was parameterized as a function of the kinetic proton energy, the actual T_{kin} reflects the proton quasi kinetic energy even in the case of a deuteron beam and a proton target.

The consequence of the above-mentioned momentum distribution is that the dp reaction results in a “smeared” pn reaction c.m. energy and enables thus sub-threshold η production [25, 26, 27]. The formation of pn composites below any threshold of the final state (as e.g. for the $pn \rightarrow pn\eta$ threshold) is rejected while counting the number of rejected events to keep the proper normalization.

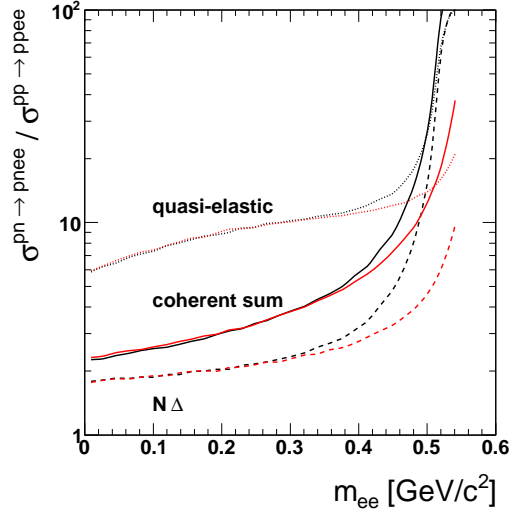


Figure 4: Ratio of $\sigma^{pn \rightarrow pnee} / \sigma^{pp \rightarrow ppee}$ as a function of m_{ee} using the OBE calculation [11] with the resonant $N\Delta$ term (dashed curves), the quasi-elastic term (dotted curves) and the full calculation (solid curves), for a beam energy of 1.25 GeV/u. The grey (online: red) curves are obtained with the pure pn reaction, whereas the black curves include the momentum distribution of the deuteron.

Fig. 3 shows the different channels which are combined later on in the final di-electron cocktails.

3.5 pn/pp ratio

In the following, the iso-spin dependence of the bremsstrahlung is discussed. By using the same methods for the OBE calculations for the resonant term, the quasi-elastic term and the full calculation, respectively, and dividing the simulation results for pn and pp the iso-spin dependence can be studied. Fig. 4 shows this ratio for the different contributions and the coherent sum, optionally including the momentum distribution of the deuteron. The simulation indicates that the influence of the momentum distribution for masses smaller than 0.4 GeV/c^2 is negligible.

3.6 Cocktail simulation

In the context of the new HADES data, the simulation has to be done with a full cocktail calculation. Here, all channels contributing to di-electron production at given energy have to be included. The main source of the di-electrons are the π^0 Dalitz decays. The production of π^0 mesons is done within the Δ resonance model assuming that all π^0 's are created via Δ . The production of η mesons is also included for the dp case.

Fig. 5 shows the possible contributions for the di-electron production, based on (i) the model from refs. [11, 12], and (ii) on the Δ production and subsequent Dalitz decay. The difference

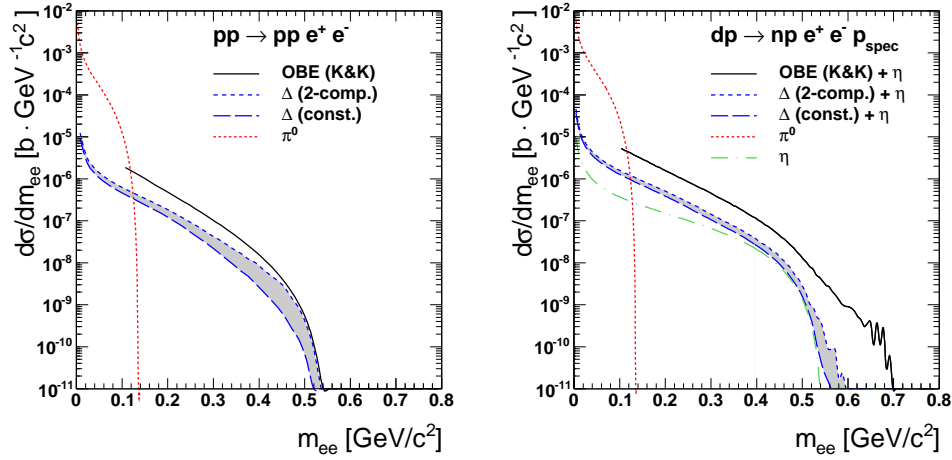


Figure 5: (color online) Cocktail simulation of the differential cross section of $d\sigma/dm_{ee}$ for the pp reaction at 1.25 GeV (left) and the dp reaction at 1.25 GeV/u (right). Long dashed (blue) curve: Δ Dalitz decay using constant transition form factors, short dashed (blue) curve: same with the two component quark model from [22, 40], solid black curve: full coherent OBE calculation from [11], dot-dashed (red) curve: π^0 Dalitz decay, dotted (green) curve: η Dalitz decay (dp only). In the dp case, the η contribution has been added to the short-lived components.

between these two approaches is clearly visible. Moreover, the Dalitz decay is used with the form factor model from Iachello and Wan [22].

We expect that the HADES data will be sensitive to differences in the various descriptions. However, the simulation done with the Pluto framework has to be filtered first with the acceptance of the HADES spectrometer. One limitation is here that the OBE calculations [11, 12, 13] provide only the invariant mass spectra, but do not show predictions for angular distributions. In the Δ Dalitz decay model from Pluto, however, these effects are taken into account using existing data [15]. We therefore would like to suggest that future theoretical investigations should consider and present these distributions as this would be extremely helpful for the disentanglement as well as understanding of the aforementioned effects, specifically concerning the HADES data.

4 Summary

In summary we have presented the details of an extension of the previous Pluto framework able to incorporate important descriptions for the production of low-mass di-electrons in elementary collisions such as pp and quasi-free pn . Several models based on a free Δ Dalitz decay and full quantum mechanical calculations have been included so far and are ready for the comparison with the upcoming HADES data [8]. As the intermediate excitation of Δ is important for the di-electron production, we have described in detail the corresponding models.

Acknowledgments

We greatly appreciate fruitful discussion with F. Iachello about the two-component model and thank for the permission to use his calculations in our event generator. Furthermore, the authors would like to thank R. Shyam for the support of a new set of calculations compatible to the HADES energies. Interesting discussions with U. Mosel are greatly appreciated.

This work was supported by the Hessian LOEWE initiative through the Helmholtz International Center for FAIR (HIC for FAIR) and by the Helmholtz Alliance EMMI “Extremes of Density and Temperature: Cosmic Matter in the Laboratory”, and BMBF 06DR135.

A Δ Dalitz decay models

A.1 Differential decay width of the Δ Dalitz decay

In this report, for computing the $\Delta(1232)$ Dalitz decay we use the prescription of Ref. [34]

$$\frac{d\Gamma_{m_\Delta}^{\Delta \rightarrow N e^+ e^-}}{dm_{ee}}(m_{ee}) = \frac{2\alpha}{3\pi m_{ee}} \Gamma_{m_\Delta}^{\Delta \rightarrow N \gamma^*}(m_{\gamma^*} \equiv m_{ee}). \quad (26)$$

with $\alpha = 1/137$ as the fine structure constant. The decay process $\Delta \rightarrow N \gamma^*$ consists in three independent amplitudes, which can be calculated unambiguously from the electromagnetic vertex. However, as stressed in [24], inconsistent formula for the differential decay width of this process can be found in the literature. We tackled the calculation by ourselves, using the magnetic dipole, electric quadrupole and Coulomb quadrupole covariants [35], and could confirm the expression of [24], as repeated below:

$$\begin{aligned} \Gamma_{m_\Delta}^{\Delta \rightarrow N \gamma^*}(m_{\gamma^*}) &= (G_{m_\Delta}^{\Delta \rightarrow N \gamma^*}(m_{\gamma^*}))^2 \\ &\times \frac{\alpha}{16} \frac{(m_\Delta + m_N)^2}{m_\Delta^3 m_N^2} \sqrt{y_+ y_-^3}, \\ y_\pm &= (m_\Delta \pm m_N)^2 - m_{ee}^2, \end{aligned} \quad (27)$$

where the index N refers to the produced nucleon, e is the electron charge, and $G_{m_\Delta}^{\Delta \rightarrow N \gamma^*}(m_{\gamma^*})$ depends on the N - Δ electromagnetic transition form factors as

$$\begin{aligned} (G_{m_\Delta}^{\Delta \rightarrow N \gamma^*}(m_{\gamma^*}))^2 &= |G_M^2(m_{\gamma^*})| + 3 |G_E^2(m_{\gamma^*})| \\ &+ \frac{m_{\gamma^*}^2}{2m_\Delta^2} |G_C^2(m_{\gamma^*})| \end{aligned} \quad (28)$$

where $G_M(m_{\gamma^*})$, $G_E(m_{\gamma^*})$, $G_C(m_{\gamma^*})$ are the magnetic, electric and Coulomb $N - \Delta$ transition form factors, respectively, which will be discussed in the next section of the appendix. Note that eq. (27) implies a normalization of the form factors as in [35], since isospin factors are included in the numerical factors. We could also check the validity of the expressions derived in [36], where the amplitudes are calculated with a different, but equivalent set of covariants, with corresponding form factors. We use eqn. (27) throughout.

A.2 Electromagnetic $N - \Delta$ transition form factors

The electromagnetic $N - \Delta$ transition form factors are analytical functions of the squared four-momentum transfers q^2 at the $N - \Delta$ vertex. Pion electroproduction and photo production experiments allow to determine these formfactors in the space-like region ($q^2 \leq 0$) [37]. In the Δ Dalitz decay process, due to the positive four-momentum transfer squared ($q^2 = m_{\gamma^*}^2 > 4m_{ee}^2$), the time-like region is probed, where only the limit at $q^2 = 0$ is known experimentally. An additional difficulty hails from the fact that the form factors, which are real in the space-like region, get an imaginary part in the time-like region.

Therefore, two options can be chosen to compensate the lack of experimental information on these observables and have been implemented for Pluto simulations.

A.2.1 Constant $N - \Delta$ transition form factors

In this option, which is based on the smallness of the squared four-momentum transfer q^2 in the Δ Dalitz decay process, the form-factors are given the values $G_M=3.0$, $G_E=0$, $G_C=0$. This choice is consistent with the precise measurements of the electric and magnetic form factors in pion photoproduction experiments [37] and with the very small contribution of the Coulomb term in eq. (28) and provides in addition the correct radiative decay width $\Gamma^{\Delta \rightarrow N\gamma^*} = 0.66$ MeV. The resulting branching ratio at the pole mass of $b^{\Delta \rightarrow Nee} = 4.19 \cdot 10^{-5}$ is remarkably consistent to the photon decay branching ratio times the fine structure constant α which would result in $b^{\Delta \rightarrow Nee} = 4.01 \cdot 10^{-5}$.

A.2.2 Two-component quark model

The alternative is to use a model for the $N - \Delta$ transition form factors. This model should in principle satisfy the analyticity properties in the complex q^2 plane, as well as the asymptotic behavior predicted by QCD sum rules, while reproducing the existing data measured in the space-like region. At first, the photon-point value provides the normalization of the whole function. As an example of such models, the two-component quark model, described in the following, has been implemented in the Pluto event generator.

The picture behind this transition form-factor model is the overlay of an intrinsic q^3 structure and a meson cloud which couples to the virtual photon via vector mesons [38]. The model allows an analytical continuation of the function from space-like to time-like region [39], inducing a phase, and could be successfully applied to the description of elastic space-like and time-like nucleon form-factor measurements. The formalism has been recently extended to calculate also baryonic transition form factors in a unified way [22], these new developments have been tested on the space-like $N - \Delta$ transition form factors measurements. We use here the simplest version of the model, which assumes isospin symmetry, and therefore considers only the magnetic $N - \Delta$ transition form factor. The intrinsic 3-quark structure is described as:

$$g(q^2) = \frac{1}{(1 - a^2 e^{i\theta} q^2)^2} \quad (29)$$

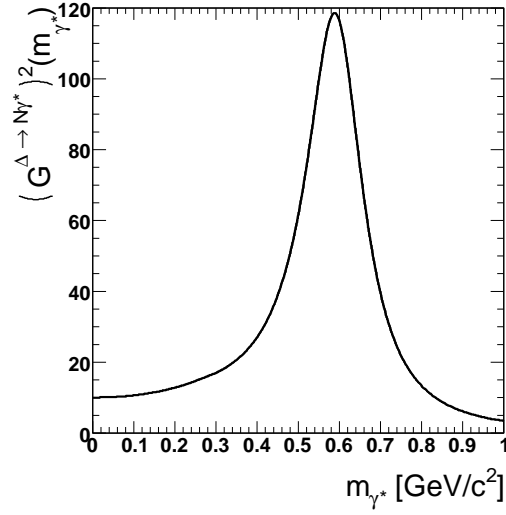


Figure 6: Form factor model taken from [22, 40].

and the overall expression for the time-like $N - \Delta$ transition form factor is:

$$G_M(q^2) = \mu_p \left(\frac{4}{3\sqrt{2}} \right) \sqrt{\frac{2m_N m_\Delta}{m_\Delta^2 + m_N^2}} g(q^2) \times (\beta' + \beta F_\rho(q^2)), \quad (30)$$

where $\mu_p = 2.793$ is the proton magnetic moment and β and β' are the constants for the coupling to the quark core and to the meson-cloud respectively. In the case of the $N - \Delta$ transition, only the ρ meson contributes to the latter contribution, due to isospin conservation and the corresponding q^2 -dependence is given by $F_\rho(q^2)$, as:

$$F_\rho(q^2) = \frac{m_\rho^2 + 8\Gamma_\rho m_\pi / \pi}{m_\rho^2 - q^2 + 4m_\pi(1-x)\Gamma_\rho(\alpha(x) - i\gamma(x))}, \quad (31)$$

where we have introduced $x = q^2/4m_\pi^2$ and [40]

$$\left. \begin{aligned} \alpha(x) &= \frac{2}{\pi} \sqrt{\frac{x-1}{x}} \ln(\sqrt{x-1} + \sqrt{x}) \\ \gamma(x) &= \sqrt{\frac{x-1}{x}} \end{aligned} \right\} \text{if } x > 1 \quad (32)$$

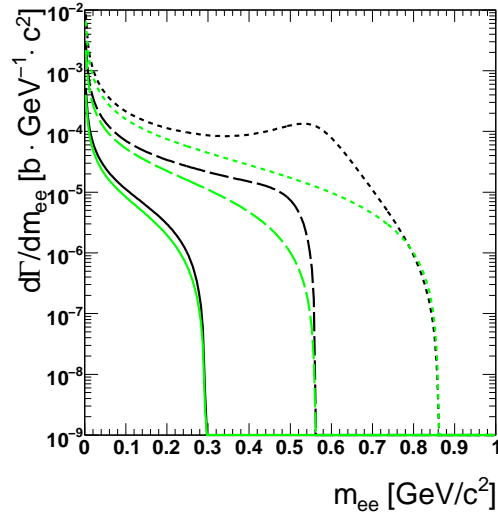


Figure 7: (color online) The distribution $\frac{d\Gamma_{m_\Delta \rightarrow Ne^+e^-}(m_{ee})}{dm_{ee}}$ as a function of m_{ee} for 3 different Δ masses. Solid curves: pole mass $m_\Delta = 1.232$ GeV, long dashed curves: $m_\Delta = 1.5$ GeV and short dashed curves: $m_\Delta = 1.8$ GeV. The description from [24] is applied. The upper set of black curves has been calculated with the two-component quark model from ref. [22] whereas the lower set of grey (online: green) have been obtained with the constant transition amplitudes as described in the text.

$$\left. \begin{aligned} \alpha(x) &= \sqrt{\frac{1-x}{x}} \left[1 - \frac{2}{\pi} \cot^{-1} \sqrt{\frac{x}{1-x}} \right] \\ \gamma(x) &= 0 \end{aligned} \right\} \text{if } x < 1. \quad (33)$$

In eq. 31, the values $m_\rho=765$ MeV and $\Gamma_\rho=112$ MeV are used different from the physical values due to the form of parameterization. The value of the parameters $a=0.29$ GeV⁻², $\theta=53^\circ$, $\beta=1.2147$ and $\beta'=0.004$ results from fits of the model predictions to the available experimental information as discussed above. The resulting distribution of form-factor values (see fig. 6) shows a broad peak centered around $\sqrt{q^2} = m_{ee} \sim 0.6m_\rho^2$. Due to the small value of the β' parameter, the contribution of the coupling to the quark core in this model is negligible up to $q^2=5$ (GeV/c)², the dominant feature of the model in the kinematic range probed by the Dalitz decay process is therefore the vector dominance.

Fig. 7 finally shows the distribution $d\Gamma_{m_\Delta \rightarrow Ne^+e^-}/dm_{ee}$ for the two form factor models. The results clearly exhibit a rising decay width for larger Δ masses. In a proton-proton collision at 1.25 GeV incident energy, the mass of the produced baryonic resonance is limited to 1.48 GeV/c², the latter effect will nevertheless affects the shape of the di-electron mass spectrum shown in Sec. 3.2. The Δ Dalitz decay branching ratio, defined at the pole mass is however

mainly determined by the values of the form factor at very low q^2 . The branching ratio obtained using the two-component quark model form factor is about 10% larger than with the constant “photon-point” value, as discussed in A.2.1. This derives from the fact that the parameters of the model are fitted to a set of data over a large q^2 range, which results in a slightly too high value for the magnetic form factor at $q^2 = 0$.

One should note that, in the semi-classical description, this would correspond to the production of an on-shell ρ meson, which should therefore not be added then as an independent contribution when enabling the two-component quark model.

References

- [1] G. Agakishiev *et al.* [HADES Collaboration], Eur. Phys. J. A, in print, [arXiv:0711.4281 [nucl-ex]].
- [2] K. Schmidt, E. Santini, S. Vogel, C. Sturm, M. Bleicher, H. Stöcker, Phys. Rev. C **79** (2009) 064908 [arXiv:nucl-th/0811.4073]; E. Santini, M.D. Cozma, A. Faessler, C. Fuchs, M.I. Krivoruchenko, B. Martemyanov, [arXiv:nucl-th/0811.2065]; E. Santini, M.D. Cozma, A. Faessler, C. Fuchs, M.I. Krivoruchenko, B. Martemyanov, Phys. Rev. C **78** (2008) 034910; M. Thomere, C. Hartnack, Gy. Wolf, J. Aichelin, Phys. Rev. C **75** (2007) 064902; H.W. Barz, B. Kämpfer, Gy. Wolf, M. Zetenyi, [arXiv:nucl-th/0605036].
- [3] E. L. Bratkovskaya and W. Cassing, Nucl. Phys. A **807** (2008) 214 [arXiv:0712.0635 [nucl-th]].
- [4] G. Agakishiev *et al.* [HADES Collaboration], Phys. Rev. Lett. **98**, 052302 (2007) [arXiv:nucl-ex/0608031].
- [5] G. Agakishiev *et al.* [HADES Collaboration], Phys. Lett. B **663** (2008) 43 [arXiv:0711.4281 [nucl-ex]].
- [6] M. Schäfer, H. C. Dönges, A. Engel, U. Mosel, Nucl. Phys. A **575** (1994) 429 [arXiv:nucl-th/9401006].
- [7] K. Lapidus *et al.* [HADES Collaboration], arXiv:0904.1128 [nucl-ex],
- [8] G. Agakishiev *et al.* [HADES Collaboration], to be published.
- [9] H. C. Dönges, M. Schäfer, U. Mosel, Phys. Rev. C **51** (1995) 950 [arXiv:nucl-th/9407012]; M. Schäfer, H. C. Dönges, U. Mosel, Phys. Lett. B **342** (1995) 13 [arXiv:nucl-th/9408013].
- [10] F. de Jong and U. Mosel, Phys. Lett. B **392** (1997) 273 [arXiv:nucl-th/9611051].
- [11] L. P. Kaptari and B. Kämpfer, Nucl. Phys. A **764** (2006) 338 [arXiv:nucl-th/0504072].
- [12] L. P. Kaptari and B. Kämpfer, arXiv:0903.2466 [nucl-th].

- [13] R. Shyam and U. Mosel, Phys. Rev. C **67** (2003) 065202 [arXiv:hep-ph/0303035]; R. Shyam and U. Mosel, arXiv:0811.0739 [hep-ph].
- [14] C. Gale and J. I. Kapusta, Phys. Rev. C **40** (1989) 2397; K. L. Haglin, Annals Phys. **212** (1991) 84.
- [15] I. Fröhlich *et al.*, PoS(ACAT)076 [arXiv:0708.2382 [nucl-ex]].
- [16] <http://root.cern.ch>
- [17] GEANT3 Detector description and simulation tool, CERN long writeup W5013 (1993).
- [18] I. Fröhlich *et al.*, arXiv:0905.2568 [nucl-ex].
- [19] S. Teis, W. Cassing, M. Effenberger, A. Hombach, U. Mosel, Gy. Wolf, Z. Phys. A **356** (1997) 421.
- [20] Gy. Wolf, G. Batko, W. Cassing, U. Mosel, K. Niita, M. Schäfer, Nucl. Phys. A **517** (1990) 615.
- [21] J.H. Koch, N. Ohtsuka, J. Moniz, **154** (1984) 99.
- [22] Q. Wan and F. Iachello, Int. J. Mod. Phys. A **20** (2005) 1846; Q. Wan, Ph.D. Thesis, Yale University, New Haven, Connecticut (2007); F. Iachello, priv. comm. (2008).
- [23] L.G. Landsberg, Phys. Rep. **128**, 301 (1985).
- [24] M.I. Krivoruchenko, A. Faessler, Phys. Rev. **D65** (2002) 017502 [nucl-th/0104045].
- [25] P. Moskal *et al.*, Phys. Rev. C **79** (2009) 015208 [arXiv:0807.0722 [hep-ex]].
- [26] H. Calen *et al.*, Phys. Rev. C **58** (1998) 2667.
- [27] H. Calen *et al.*, Phys. Rev. Lett. **79** (1997) 2642.
- [28] R. Shyam, priv. communication, 2008.
- [29] V. Dmitriev, O. Sushkov, C. Gaarde, Nucl. Phys. A **459** (1986) 503.
- [30] A. Sibirtsev and W. Cassing, arXiv:nucl-th/9904046.
- [31] A. I. Titov, B. Kämpfer, B. L. Reznik, Eur. Phys. J. A **7** (2000) 543 [arXiv:nucl-th/0001027].
- [32] P. Benz *et al.* Nucl. Phys. B **65** (1973) 158.
- [33] A. V. Anisovich, I. Jaegle, E. Klempt, B. Krusche, V. A. Nikonov, A. V. Sarantsev, U. Thoma, arXiv:0809.3340 [hep-ph].
- [34] G. Wolf, G. Batko, W. Cassing, U. Mosel, K. Niita, M. Schaefer, Nucl. Phys. A **517** (1990) 615.

- [35] H. F. Jones and M. D. Scadron, *Ann. Phys.* **81**, **1** (1973).
- [36] M. Zetenyi and G. Wolf, *Heavy Ion Phys.* **17**, 27 (2003) [arXiv:nucl-th/0202047].
- [37] V. Pascalutsa, M. Vanderhaeghen and S. N. Yang, *Phys. Rept.* **437**, 125 (2007) [arXiv:hep-ph/0609004].
- [38] F. Iachello, A. D. Jackson, A. Lande, *Phys. Lett. B* **43** (1973) 191.
- [39] F. Iachello and Q. Wan, *Phys. Rev. C* **69** (2004) 055204.
- [40] F. Iachello, Yale University, internal report, Dez. 2008.